
Self-supervised Crack Detection in X-ray Computed Tomography Data of Additive Manufacturing Parts

Anonymous Author(s)

Affiliation

Address

email

Abstract

1 Following the current trends for minimizing human intervention in training intelli-
2 gent architectures, this paper proposes a self-supervised method for quality control
3 of Additive Manufacturing (AM) parts. An Inconel 939 sample is fabricated with
4 the Laser Powder Bed Fusion (L-PBF) method and scanned using X-ray Computed
5 Tomography (XCT) to reveal the internal cracks. A self-supervised approach was
6 adopted by employing three modules that generate crack-like features for training
7 a CycleGAN network. The proposed method generates random cracks based on a
8 combination of uniform and normal random variables and outperforms the others
9 in fine-grain crack detection and capturing narrow tips. A preliminary investigation
10 of the training process shows that the algorithm has the capability of predicting the
11 crack propagation direction as well.

12 1 Introduction

13 Additive Manufacturing (AM) is one of the pillars of Industry 4.0 and defined as “the general term
14 for those technologies that successively join material to create physical objects as specified by 3D
15 model data” [1]. The term “additive” emphasizes its distinction from subtractive and formative
16 methods, wherein the desired component is obtained by cutting or shaping raw materials. AM enables
17 rapid prototyping, customized production, and localized manufacturing, which revolutionizes sectors,
18 such as aerospace, automotive, healthcare, and construction. However, the inherent layer-by-layer
19 fabrication process of AM is likely to introduce internal volumetric features in the final product,
20 such as cracks and pores. These features are closely linked to the processing parameters, physical
21 properties, and mechanical characteristics of the manufactured part.

22 In the quest to make AM parts with superior qualities, mining the correlation between the processing
23 parameters, internal features, and mechanical properties of the final part is a huge progress. Currently,
24 all fabrication, evaluation, and testing stages rely on digital devices, resulting in the generation
25 of large amounts of data throughout the process. The advent of AI, in conjunction with powerful
26 computational devices, has ushered in fresh opportunities to accomplish this mission through data-
27 driven approaches.

28 Within the data-driven formulation, the non-destructive evaluation (NDE) assumes a pivotal role in
29 assessing the internal features of the part fabricated with a given set of processing parameters. Among
30 various NDE methods, X-ray Computed Tomography (XCT) has demonstrated exceptional efficacy
31 in revealing internal defects due to its accessibility, high resolution, and ability to detect features at
32 the micron level. The XCT analysis yields a stack of 2D slices that together create a 3D volume,
33 which must be quantified to determine the volume fraction associated with each type of defect. This
34 process can be described as a *semantic segmentation* task in the context of computer vision.

35 At the top level, segmentation methods can be divided into manual and automated methods. In
36 manual methods, a human expert annotates the entire stack of images by assigning distinct regions
37 to a particular class with an image editor. The expert’s judgment typically has the highest level
38 of accuracy and reliability. However, they have limited tools (e.g. poor eyesight, shaky mouse
39 pointer, losing focus) to translate their abstract judgment into pixel-level-accurate segmentation maps.
40 Moreover, it takes a considerable amount of time, energy, money, and manpower to quantify the
41 entire volume.

42 Automated methods are a set of tools that the expert can use to accelerate the segmentation process.
43 These methods encompass a wide range of techniques, from simple image processing to advanced
44 parametric approaches inspired by statistical learning and artificial intelligence. Traditionally, statisti-
45 cal models were trained by hand-craft features, which demanded significant expertise, time, and
46 effort to decipher hidden information inside the raw data to be used as training data. The advent of
47 deep learning techniques, such as DeepLabV3 [2] and Mask R-CNN [3], eliminates the need for
48 hand-crafted features but requires extensive volumes of labeled data.

49 Most of the state-of-the-art solutions have focused on the complexity of the architecture and designing
50 algorithms that are able to learn the contextual information inside the training data. However, in the
51 context of additive manufacturing fault detection, it is shown that the reliability of the training data
52 is the bottleneck that limits the performance of AI-based networks [4]. Therefore, in this work, our
53 major goal is to eliminate the manually labeled data to reduce our dependency on human experts and
54 avoid producing erroneous training data. Instead, we present a module that can generate random
55 crack-like features that can serve as manually labeled data. Our contributions include:

- 56 • Eliminating the manual segmentation process and the corresponding uncertainties
- 57 • Achieving fine-grain crack tip detection
- 58 • Getting one step closer to the physics-informed prediction of crack propagation

59 This idea can ensure fine-grained detection of cracks and microcracks inside X-ray CT data. Our
60 results show this idea not only enables precise identification of cracks and microcracks within X-ray
61 CT data but also has the capability to forecast the direction in which crack propagation occurs. This
62 can be further improved by incorporating the physical governing equations into the crack generation
63 algorithm.

64 **2 Related Work and Background**

65 The supervised learning approach is the most common approach in semantic segmentation, as it
66 has a well-established framework. In this method, training data is prepared manually by human
67 domain experts. Among all supervised methods, U-Net [5] was a breakthrough in medical image
68 segmentation due to the efficient aggregation of high-resolution and low-resolution features. More
69 efforts have been made to trade off between global and local information by developing more
70 complicated architectures [6, 7]. Vision Transformers are the most modern tools to address this
71 challenge [8]. The drawback is that these networks need a large amount of pixel-level manually
72 annotated training data. In particular, cracks tend to get narrower as they propagate and the crack tip
73 (which is the most crucial part of the crack to be detected) fades into the background, making it either
74 very hard to manually segment or ending up with unreliable training data [4].

75 One workaround to reduce the dependency on manually labeled data is to train the network on a
76 standard dataset (e.g. ImageNet) and fine-tune the weights on the target dataset, which is known as
77 Domain adaptation [9]. Nonetheless, the accuracy of the final output is still affected by the erroneous
78 target dataset.

79 Urged to propose a solution to this bottleneck, researchers have turned their attention towards semi-
80 supervised and unsupervised learning approaches to completely eliminate the manual segmentation
81 process. In a self-supervised approach through the abstraction of the domain experts’ knowledge.
82 In these methods, the model trains itself by generating labeled data, by which it transforms an
83 unsupervised problem into a supervised problem [10]. Self-supervised learning shows significant
84 potential in enhancing representations in situations where there is a limited amount of labeled data
85 [11], which is the case in AM fault detection applications.

86 In the context of Additive Manufacturing, despite its huge benefits including the capability to
87 print sophisticated structures and simplicity of use, there are challenges that need more research

88 and advancement including part size limitation, anisotropic mechanical characteristics, high cost
89 of production, demand for high-quality products, warping, pillowing, stringing, gaps in the top
90 layers, under-extrusion, layer misalignment, and over-extrusion [12]. To tackle these challenges,
91 additive manufacturing can benefit from AI in post-processing stages where the parts are already
92 built. Information extracted from AI models can be used for quality control, energy, and resource
93 management and optimize the process for future parts to be built and reduce defects such as cracks
94 and pores [13].

95 As Nemati *et al.* [4] showed, zero-shot learning approaches need to be tested in XCT quantification
96 to minimize the training data uncertainty. In this regard, Hu *et al.* used a self-supervised contrastive
97 representation for steel surface defect detection [14]. An unsupervised Out-of-Distribution data
98 detection scheme with Autoencoders was proposed by Kolektor *et al.* [15] for the same application.
99 Lindgren and Zach [16] proposed an auto-encoder deep learning approach for quality control with
100 non-destructive evaluation for out-of-distribution data. This model is used as a one-class classifier for
101 industrial X-ray images trained and tested on the public dataset Kolektor SDD. Wang [17] presented
102 a novel contrastive learning-based semantic segmentation model, named cLass-aware Semantic
103 Contrast and Attention Amalgamation to detect in-situ stratified defects and extract rich semantic
104 contexts with limited imbalanced data. In their approach, they proposed an adaptive sampling
105 approach to categorize the pixels into two groups: 1-Easy-to-detect and 2- Hard-to-detect. This
106 division aims to safeguard against inaccurate predictions in the defect memory bank during the initial
107 learning phases.

108 **3 Methodology**

109 **3.1 Overview**

110 The modern engineer is well-educated in both practical engineering and simulations. The wealth of
111 simulation tools at the engineer’s fingertips is powerful and comprehensive. This present methodology
112 merges the engineering simulation skill set with artificial intelligence starting with the relatively
113 simple simulation of 2-D crack networks. We would like to emphasize this application is the first
114 step on a path of 3-D crack simulation, crack growth simulation, and cracks through inhomogeneous
115 media. That is, the dimensionality of the training sets is projected to increase for this initial 2-D into
116 3-D, 4-D (cartesian space plus time), 5-D (cartesian space plus time plus reinforced materials), 6-D
117 (cartesian space plus time plus reinforced materials plus wear), and more (composite materials). All
118 of these situations, ordered by dimensionality, have corresponding engineering simulation tools. The
119 present work develops a path from the world of engineering simulations into the facile generation of
120 training sets for artificial intelligence.

121 The overview of the employed CycleGAN process is shown in Figure 1. We follow the same
122 architecture as [18], and we put of focus on the crack generation module and its effect on the overall
123 performance of the segmentation results for XCT data of AM parts.

124 **3.2 Crack Generation Modules (CGMs)**

125 We need to populate a dataset for crack-like features to serve as segmentation maps during training in
126 a self-supervised approach. Typical cracks in AM parts have random planar structures that propagate
127 through material depending on the factors including but not limited to composition, processing
128 parameters, build direction, and post treatments. In particular, Inconel 939 fabricated using the L-PBF
129 method is likely to contain solidification cracks, liquation cracks, ductility-dip cracks, and strain-age
130 cracks [19]. However, it is practically impossible to find a closed-form deterministic function to
131 estimate the crack morphology due to numerous unknown factors and uncertainties. Therefore, we
132 tested 3 different Crack Generation Modules (CGMs) to populate crack-like datasets:

- 133 • CGM1: Synthetic simplified fractal generator module proposed by [18].
- 134 • CGM2: Experimental concrete crack dataset available online. [20, 21]
- 135 • CGM3: Synthetic random crack generator proposed by us.

136 The first module (CGM1) generates fractals based on rectangular units in a sequential order to
137 simulate coronary angiogram images. The details can be found in the original paper [18]. We utilized

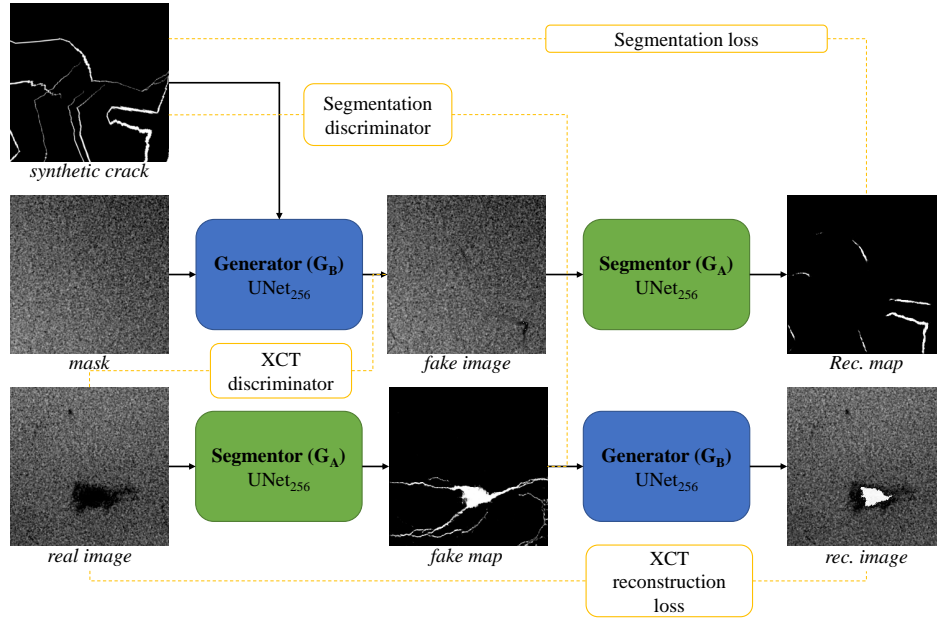


Figure 1: The workflow of the CycleGAN network during training. The data flow for map reconstruction and image reconstruction is independent. However, the loss functions take input from both paths, forcing them to converge simultaneously. In the testing phase, only the trained Segmenter G_A is used for generating the segmentation map from a real image.

138 the exact same module to evaluate the effectiveness of this algorithm in AM crack detection. The
 139 second module (CGM2) is an experimental dataset containing aerial images of concrete cracks that
 140 are manually segmented by domain experts [20, 21]. These cracks show similar morphologies to
 141 typical AM cracks with some differences. We used this module to assess the performance of an
 142 existing empirical dataset from a different application, which needs minimal data preparation. Our
 143 final endeavor to simulate crack-like features involves the introduction of a synthetic random crack
 144 generator (CGM3), which is explained below.

145 **Synthetic Random Crack Generator.** To simulate the morphology of typical cracks in 2D slices
 146 of AM parts, we used different random variable generators that sample from uniform and normal
 147 distributions to initialize the crack dimensions. First, the center of the crack is sampled from
 148 the uniform distribution $(C_{x,0}, C_{y,0}) \sim \mathcal{U}_c((0, 0), (ps, ps))$, where ps stands for the size of an
 149 equidimensional patch. Once the center of the crack is determined, a horizontal crack profile can be
 150 generated by stacking a sequence of vertical lines with decaying lengths on both sides. The initial
 151 (and maximum) thickness of the crack is sampled from a uniform distribution (Equation 1). The
 152 horizontal crack is propagated from left and right by stacking more vertical lines. To mimic the
 153 irregular geometry of cracks, the lengths of successive vertical lines are calculated based on the
 154 recursive sequence (Equation 2), and a normal random variable is added to the centerline (Equation
 155 3).

$$t_0 \sim \mathcal{U}_t(t_{min}, t_{max}) \quad (1)$$

$$t_{i,side} = t_{i-1,side} \times (1 - |t \sim \mathcal{N}(0, DF)|), \quad i = 1, 2, \dots \quad (2)$$

$$C_{y,i,side} = C_{y,i-1,side} + y \sim \mathcal{N}(0, SF), \quad i = 1, 2, \dots \quad (3)$$

156 where t_{min} and t_{max} are minimum and maximum initial crack thicknesses that may exist in the part
 157 and come from the physical understanding of an expert. $side$ can be either left or right, and DF

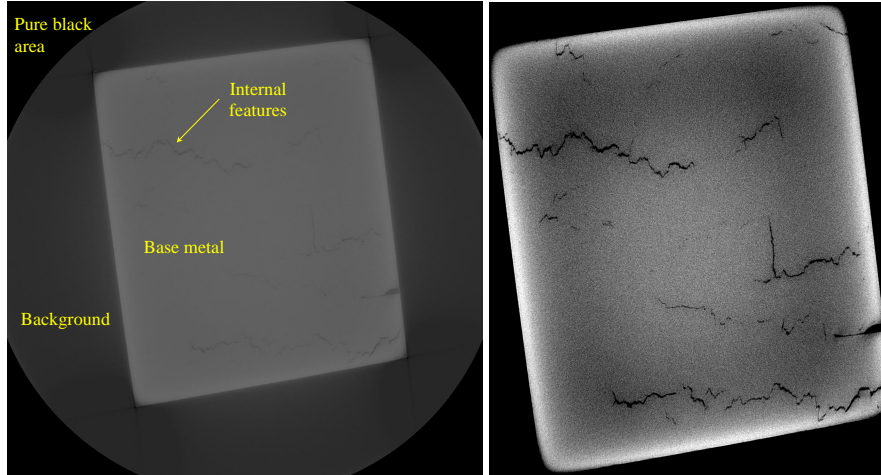


Figure 2: *Left:* an unprocessed 2624×2624 cross-section of the Inconel 939 XCT volume; the cross-section is a 16-bit grayscale image; *right:* the cropped and readjusted image; the cropped image is 1590×1872 in this figure.

158 stands for Decay Factor. The smaller the DF , the greater the crack length. The vertical position of
 159 the center point of the i th line is denoted by $C_{y,i}$, and SF stands for Smoothness Factor. Larger SF s
 160 will generate more jagged cracks. The same procedure would generate vertical cracks by stacking
 161 horizontal lines along the y axis. For each patch, a number of horizontal and vertical cracks are
 162 generated and then an augmentation operation is performed similar to the one proposed by [18]. An
 163 example of the final patch containing the synthetic cracks is shown in Figure 3(right).

164 4 Evaluation

165 4.1 Evaluation settings

166 4.1.1 Dataset

167 The experimental dataset studied in this paper is the 3D virtualization of a 2×2×5 mm³ Inconel
 168 939 bar fabricated by Laser Powder Bed Fusion (L-PBF) additive manufacturing method scanned
 169 by Thermo Fisher HeliScan microCT. The details about the fabrication conditions and processing
 170 parameters are described elsewhere [22]. The tomography volume contains 2624×2624×7868 voxels,
 171 each with 0.71 microns in size. Each cross-sectional slice is a 2624×2642 16-bit grayscale image,
 172 each contains the pure black out-of-window area, the background, the base metal, and the internal
 173 features (Figure 2(left)). The internal features are mostly 2D cross-sections of planar cracks in 3D,
 174 alongside occasional occurrences of small pores.

175 4.1.2 Data preparation

176 Since the focus is on detecting the features within the base metal, we crop the images to a smaller frame
 177 that only encompasses the sample as closely as possible. Then, the image brightness and contrast
 178 are readjusted to increase the difference between the areas with high and low X-ray attenuation.
 179 (Figure 2(right)).

180 We trained the architecture with the proposed CGMs described in Section 3.2. A few samples of the
 181 generated crack-like features are shown in Figure 3. Each cropped image is divided into 256×256
 182 non-overlapping patches for populating the dataset. We used the slices containing cracks for mask
 183 frames. Since there is no separate view of the exact same frame with the absence of crack features
 184 available, we chose another patch from the same slice with only base metal and no cracks. Although
 185 this frame does not exactly correspond to the mask image, it is presumed to have the same statistical
 186 features as the background. This assumption is valid as Ma *et al.* [18] showed this algorithm is robust
 187 to unpaired mask and contrast frames.

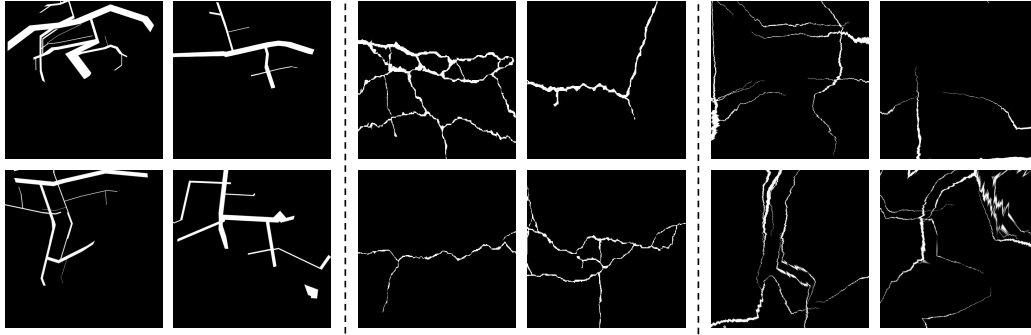


Figure 3: *Left:* synthesized fractal features [18]; *middle:* concrete crack masks [20, 21]; *right:* random crack generation with $SF = 0.01$ and $DF = 1$.

188 4.1.3 Training and Metrics

189 We implemented the architecture in the PyTorch [23] with CUDA compatibility. The assigned
 190 computational node has one NVIDIA V100S GPU, with 32 GB of memory. The optimizer is Adam
 191 [24], and the mean square error criterion is chosen as the GAN loss. The UNet-256 generator
 192 and PatchGAN discriminator modules shown in Figure 1 have 54.4 and 2.76 million parameters,
 193 respectively.

194 4.2 Results

195 We trained and tested the CycleGAN network with all the candidate CGMs and evaluated the results
 196 visually in Figure 4. Based on the results, the synthesized fractal features (CGM1) cannot represent
 197 the mechanical cracks as the network is nowhere close to generating satisfactory segmentation results.
 198 On the other hand, the datasets generated by the concrete crack (CGM2) and synthetic crack (CGM3)
 199 modules successfully conveyed the necessary contextual information which is successfully captured
 200 by the cycleGAN architecture. A closer look at the results shows that the network trained by concrete
 201 cracks tends to look for thicker cracks and miss the narrow tips. Conversely, the network trained
 202 by synthetic cracks actively looks for and identifies narrow tips of the cracks, which has a huge
 203 importance in predicting fatigue life. However, focusing on narrow features comes at the price
 204 of discontinued segmentation of thick features, which can be resolved by a set of erosion/dilation
 205 operations.

206 Another observation during training was that the architecture tends to not only find the narrow tips
 207 of the cracks but also predict the crack propagation paths (Figure 5). This means if we incorporate
 208 the physical and thermodynamics equations that determine the granular and intergranular behavior
 209 of the material into the crack generation module, we may be able to estimate the crack propagation
 210 direction based on theoretical equations. However, this claim needs to be validated by loading the
 211 part under a certain direction to force the target crack to propagate, which is left for future research.

212 5 Conclusion

213 This work evaluates the potentials of self-supervised learning in defect quantification of Additive Man-
 214 ufacturing (AM) parts scanned by X-ray Computed Tomography (XCT). An Inconel 939 fabricated
 215 using the Laser Powder Bed Fusion (L-PBF) method, which contains cracks is taken as an example.
 216 In an attempt to address the uncertainty of the training data, a self-supervised approach along with a
 217 random crack generation module is proposed to eliminate the need for manually segmented images.
 218 The experiments show that the proposed method generates promising results in terms of detecting
 219 the fine-grained crack features and capturing the narrow tips, which are critical in assessing fatigue
 220 life. Moreover, investigating the training process has shown some potential for predicting the crack
 221 propagation paths by incorporating physics-based rules into the training phase.

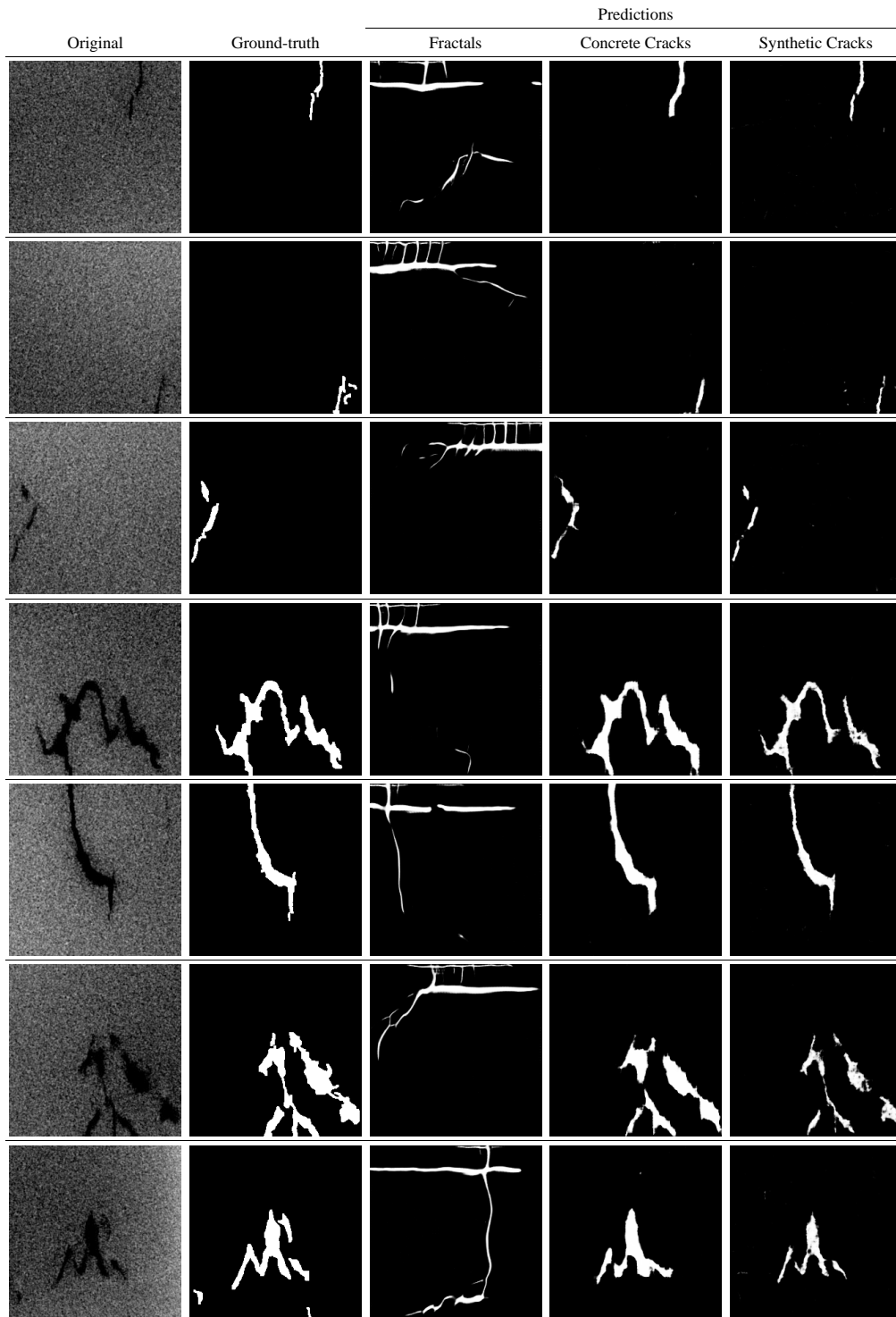


Figure 4: Comparing the segmentation results with different CGMs.

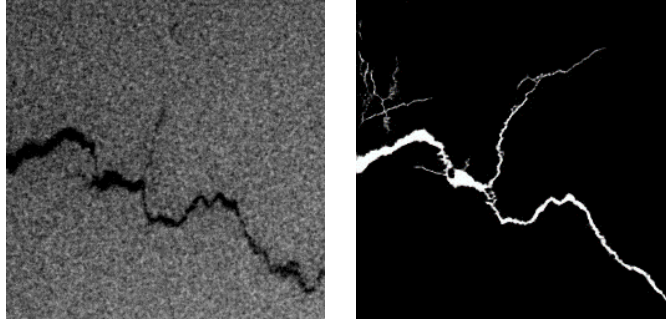


Figure 5: Evaluation of the segmentation results during training shows that the network tends to find the crack propagation path.

References

- 222
- 223 [1] ISO Central Secretary. Additive manufacturing — general principles — fundamentals and vocabular.
224 Standard ISO/ASTM 52900:2021, International Organization for Standardization, Geneva, CH, 2021.
- 225 [2] Liang-Chieh Chen, George Papandreou, Florian Schroff, and Hartwig Adam. Rethinking atrous convolution
226 for semantic image segmentation. *arXiv preprint arXiv:1706.05587*, 2017.
- 227 [3] Kaiming He, Georgia Gkioxari, Piotr Dollár, and Ross Girshick. Mask r-cnn. In *Proceedings of the IEEE
228 international conference on computer vision*, pages 2961–2969, 2017.
- 229 [4] Saber Nemati, Hamed Ghadimi, Xin Li, Leslie G. Butler, Hao Wen, and Shengmin Guo. Automated
230 defect analysis of additively fabricated metallic parts using deep convolutional neural networks. *Journal of
231 Manufacturing and Materials Processing*, 6(6), 2022.
- 232 [5] Olaf Ronneberger, Philipp Fischer, and Thomas Brox. U-net: Convolutional networks for biomedical
233 image segmentation. *ArXiv*, abs/1505.04597, 2015.
- 234 [6] Hengshuang Zhao, Jianping Shi, Xiaojuan Qi, Xiaogang Wang, and Jiaya Jia. Pyramid scene parsing
235 network. In *Proceedings of the IEEE Conference on Computer Vision and Pattern Recognition (CVPR)*,
236 July 2017.
- 237 [7] Liang-Chieh Chen, George Papandreou, Iasonas Kokkinos, Kevin P. Murphy, and Alan Loddon Yuille.
238 Deeplab: Semantic image segmentation with deep convolutional nets, atrous convolution, and fully
239 connected crfs. *IEEE Transactions on Pattern Analysis and Machine Intelligence*, 40:834–848, 2016.
- 240 [8] Hanguang Xiao, Li Li, Qiyuan Liu, Xiuhong Zhu, and Qihang Zhang. Transformers in medical image
241 segmentation: A review. *Biomedical Signal Processing and Control*, 84:104791, 2023.
- 242 [9] Abolfazl Farahani, Sahar Voghoei, Khaled Rasheed, and Hamid R. Arabnia. A brief review of domain
243 adaptation. In Robert Stahlbock, Gary M. Weiss, Mahmoud Abou-Nasr, Cheng-Ying Yang, Hamid R.
244 Arabnia, and Leonidas Deligiannidis, editors, *Advances in Data Science and Information Engineering*,
245 pages 877–894, Cham, 2021. Springer International Publishing.
- 246 [10] Randall Balestriero, Mark Ibrahim, Vlad Sobal, Ari Morcos, Shashank Shekhar, Tom Goldstein, Florian
247 Bordes, Adrien Bardes, Gregoire Mialon, Yuandong Tian, Avi Schwarzschild, Andrew Gordon Wilson,
248 Jonas Geiping, Quentin Garrido, Pierre Fernandez, Amir Bar, Hamed Pirsiavash, Yann LeCun, and Micah
249 Goldblum. A cookbook of self-supervised learning, 2023.
- 250 [11] Dan Hendrycks, Mantas Mazeika, Saurav Kadavath, and Dawn Song. Using self-supervised learning can
251 improve model robustness and uncertainty. *Advances in neural information processing systems*, 32, 2019.
- 252 [12] Osama Abdulhameed, Abdulrahman Al-Ahmari, Wadea Ameen, and Syed Hammad Mian. Addi-
253 tive manufacturing: Challenges, trends, and applications. *Advances in Mechanical Engineering*,
254 11(2):1687814018822880, 2019.
- 255 [13] Jian Qin, Fu Hu, Ying Liu, Paul Witherell, Charlie CL Wang, David W Rosen, Timothy W Simpson, Yan
256 Lu, and Qian Tang. Research and application of machine learning for additive manufacturing. *Additive
257 Manufacturing*, 52:102691, 2022.

- 258 [14] Xuejin Hu, Jing Yang, Fengling Jiang, Amir Hussain, Kia Dashtipour, and Mandar Gogate. Steel surface
259 defect detection based on self-supervised contrastive representation learning with matching metric. *Applied*
260 *Soft Computing*, 145:110578, 2023.
- 261 [15] Erik Lindgren and Christopher Zach. Deep-learning-based out-of-distribution data detection in visual
262 inspection images. In Norbert G. Meyendorf, Christopher Niezrecki, and Ripi Singh, editors, *NDE 4.0,*
263 *Predictive Maintenance, Communication, and Energy Systems: The Digital Transformation of NDE,*
264 volume 12489, page 1248909. International Society for Optics and Photonics, SPIE, 2023.
- 265 [16] Erik Lindgren and Christopher Zach. Deep-learning-based out-of-distribution data detection in visual
266 inspection images. In Norbert G. Meyendorf, Christopher Niezrecki, and Ripi Singh, editors, *NDE 4.0,*
267 *Predictive Maintenance, Communication, and Energy Systems: The Digital Transformation of NDE,*
268 volume 12489, page 1248909. International Society for Optics and Photonics, SPIE, 2023.
- 269 [17] Kang Wang. Contrastive learning-based semantic segmentation for in-situ stratified defect detection in
270 additive manufacturing. *Journal of Manufacturing Systems*, 68:465–476, 2023.
- 271 [18] Yuxin Ma, Yang Hua, Hanming Deng, Tao Song, Hao Wang, Zhengui Xue, Heng Cao, Ruhui Ma, and
272 Haibing Guan. Self-supervised vessel segmentation via adversarial learning. In *Proceedings of the*
273 *IEEE/CVF International Conference on Computer Vision (ICCV)*, pages 7536–7545, October 2021.
- 274 [19] Qingsong Wei, Yinkai Xie, Qing Teng, Mu Wen Shen, Shan Shan Sun, and Chao Cai. Crack types,
275 mechanisms, and suppression methods during high-energy beam additive manufacturing of nickel-based
276 superalloys: A review. *Chinese Journal of Mechanical Engineering: Additive Manufacturing Frontiers*,
277 2022.
- 278 [20] Kangcheng Liu, Xiaodong Han, and Ben M Chen. Deep learning based automatic crack detection and
279 segmentation for unmanned aerial vehicle inspections. In *2019 IEEE International Conference on Robotics*
280 *and Biomimetics (ROBIO)*, number <https://ieeexplore.ieee.org/document/896>, pages 381–387. IEEE, 2019.
- 281 [21] Kangcheng Liu and Ben M Chen. Industrial uav-based unsupervised domain adaptive crack recognitions:
282 From system setups to real-site infrastructural inspections. *IEEE Transactions on Industrial Electronics*,
283 2022.
- 284 [22] Bin Zhang, Huan Ding, Andrew C. Meng, Saber Nemati, Shengming Guo, and W.J. Meng. Crack reduction
285 in inconel 939 with si addition processed by laser powder bed fusion additive manufacturing. *Additive*
286 *Manufacturing*, 72:103623, 2023.
- 287 [23] Adam Paszke, Sam Gross, Francisco Massa, Adam Lerer, James Bradbury, Gregory Chanan, Trevor
288 Killeen, Zeming Lin, Natalia Gimelshein, Luca Antiga, Alban Desmaison, Andreas Köpf, Edward Yang,
289 Zach DeVito, Martin Raison, Alykhan Tejani, Sasank Chilamkurthy, Benoit Steiner, Lu Fang, Junjie Bai,
290 and Soumith Chintala. Pytorch: An imperative style, high-performance deep learning library. *ArXiv*,
291 [abs/1912.01703](https://arxiv.org/abs/1912.01703), 2019.
- 292 [24] Diederik P. Kingma and Jimmy Ba. Adam: A method for stochastic optimization. *arXiv*, 1412.6980, 2017.